scientific reports

Check for updates

OPEN

Experimental investigation of influence of age hardening temperature and cooling medium on tribological behaviour of aluminium/tungsten carbide metal matrix composite

Srinivasan Rajaram[1]✉, N. S. Balaji[2], Mamdooh Alwetaishi[3] & Shashikumar Krishnan[4]✉

This work investigates the hardness and wear resistance of an Aluminum/Tungsten carbide metal matrix composite in relation to its age-hardening temperature. The composite was fabricated by stir-casting technique, and samples were cooled in a furnace, water, and atmosphere after being aged for two hours at 0 °C, 250 °C, and 450 °C. The results showed that the composite aged at 250 °C under furnace cooling achieved a 50.48% increase in hardness compared to the non-aged composite, while those cooled under water and atmospheric conditions exhibited increases of 30.82% and 39.33%, respectively. In the investigation of the composite's wear characteristics, two variables were considered: sliding distance (1000, 1500, and 2000 m) and load (10, 20, and 30 N). The composite aged at 250 °C demonstrated a significant increase in wear resistance, attributed to high volume of precipitates formed at the grain boundaries, which reduce dislocation movement and result in reduced wear compared to other aged composites cooled under water and atmospheric conditions. The Taguchi method was used for optimization to identify conditions that minimize wear rates across various cooling environments, which were then experimentally investigated. The results revealed that low wear observed in composite aged at 250 °C, regardless of the cooling medium. For furnace-cooled samples, aged at 250 °C with a 10 N load and a 1000 m sliding distance was optimal compared to the other cooling environments and Scanning Electron Microscope (SEM) observations indicated that adhesive wear is the primary wear mechanism, with severity influenced by load, sliding distance and aging temperature.

Keywords Wear rate, Age hardening, Intermetallics, Cooling medium, Wear parameters

In the current scenario, the automotive and aerospace sectors have actively sought lightweight materials to enhance the performance of components designed for specific applications. Aluminum, celebrated for its favorable strength-to-weight ratio, stands out as a promising candidate. The increased strength and durability of Al6082-T6/SiC/B_4C composites arise from evenly distributed TiC particles, finer grain structure, and dislocation effects[1]. Employing the stir casting technique, this composite is fabricated, revealing an escalation of wear rate by increasing of sliding distance and applied load[2]. In the realm of alloy aging, optimal results are achieved at 120 °C, as evidenced by increased hardness in Al6082-T6/SiC/B4C composites[3]. Stir casting is again employed to produce AA 6061 matrix titanium carbide composites, and it is observed that wear rates rise proportionally with higher percentages of TiC, velocity, and applied load[4]. In the case of Al7075/WC composites, age hardening at 250 °C enhances wear resistance and peak hardness compared to non-aged counterparts[5].

[1]Department of Mechanical Engineering, SRM Valliammai Engineering College, Chennai 603203, India. [2]Department of Mechanical Engineering, SRM Institute of Science and Technology, Tiruchirappalli Campus, Tiruchirappalli 621105, India. [3]Department of Civil Engineering, College of Engineering, Taif University, P.O. Box 11099, Taif 21944, Saudi Arabia. [4]Faculty of Artificial Intelligence and Engineering (FAIE), Multimedia University, Persiaran Multimedia, Cyberjaya 63100, Selangor, Malaysia. ✉email: sugasri2010@gmail.com; shashikumar@mmu.edu.my

The use of Al6061 as the matrix material, with SiC, Al_2O_3, and cerium oxide as reinforcements, results in extruded composites exhibiting superior microhardness. The outcomes were found in minimal wear rates at various running conditions[6]. This progression underscores the constant quest within materials science for innovative solutions to augment the performance of components in demanding environments. The maximum tensile strength increased by the precipitation during the aging of the composite. The Ti particles interface with the matrix alloy is strengthened due to the formation of the $TiAl_3$ and Mg-Ti layer, causing Ti particles to receive much more effective strengthening effects, which improve the strength and ductility[7]. AA6061/Al_2O_3/SiC composites fabricated using the squeeze casting process exhibit wear properties that are more significantly influenced by the applied load compared to speed and sliding distance[8]. The empirical findings underscore that among the determinants influencing abrasive wear, the grain size of the abrasive emerges as primary factor, with subsequent significance attributed to the dimensions of the reinforcement, as elucidated in reference[9]. The fabrication of composites involved the utilization of AA2219 Aluminium alloy, incorporating molybdenum di sulphide (MoS_2) via the stir casting technique, wear resistance significantly decreased while lubricated by tire oil[10]. TiC particles of 35 µm were added to the molten aluminum matrix (A356) to form the composite material, which was then subjected to age hardening at 155 °C for 3 h. The conclusion of the study indicates that the undissolved precipitates form an intermediate phase, thereby enhancing the strength of composite[11]. The wear coefficient of hard silicon nitride added aluminium alloy decreases because of the mechanically mixed layer[12]. Using a powder metallurgy approach; the composite was manufactured with different SiC and B_4C weight percentages. The output of the hybrid composite can be significantly increased strength by incorporating of SiC and B_4C into the aluminum matrix[13]. Applied load and sliding distance are key factors affecting wear in composites, with wear increasing as load and sliding distance increase[14].

The aluminum hybrid composite was developed using SiC and Al2O3 as reinforcements. As sliding distance increases, the temperature of the contact surfaces rises, leading to the softening of the pin surface in contact with the disc. This results in substantial deformation and a significant increase in the volumetric wear loss of the pin[15]. Compared to other variables, such as aging temperature and aging time, it is evident that the tensile strength of the composite is more significantly impacted by the solutionizing process[16,17]. The strength of the hybrid composite improves with up to 15% reinforcement addition; however, beyond this point, the strength decreases[18]. The addition of SiC and Al2O3 particles, with 20% reinforcement, results in a hybrid composite that exhibits improved mechanical strength but no significant enhancement in impact strength[19]. The research indicated a direct correlation between wear rate and load, speed, and sliding distance, but an inverse relationship with ceramic particle addition[20].

The incorporation of steel particles enhanced the ductility of a hybrid composite fabricated via powder metallurgy using SiC and steel as reinforcements[21]. Meanwhile, the strength of the hybrid composite improved with higher additions of SiC and B_4C, attributed to the increased carbide content[22]. Similarly, elevating the weight% of silicon carbide (SiC) and aluminum oxide (Al_2O_3) in the aluminum matrix boosted the hardness and tensile strength of the hybrid nanocomposite[23]. Centrifugal casting further refined the grain size by 48.76% compared to the original microstructure, resulting in higher tensile strength, yield strength, and hardness[24]. Ali Kalkanlı et al. employed the squeeze casting method to produce an Al 7075-SiC composite, reporting that the tensile strength of the composite was lower than its flexural strength for identical SiC compositions. In another study, a hybrid composite was synthesized through powder metallurgy using SiC and kaolin particles as reinforcements. The results revealed that hardness increased with higher kaolin content in the aluminum matrix. However, when the kaolin content exceeded 4%, the tensile strength of the composite declined[25–28].

The aluminium (Al7075) alloy served as the matrix material, reinforced with tungsten carbide (WC) particles ranging in size from 3 to 5 µm. Tungsten carbide (WC) was selected for its exceptional hardness, which surpasses that of other common ceramic reinforcements such as alumina (Al_2O_3), silicon carbide (SiC), and zirconia (ZrO_2), thereby enhancing the composite's wear resistance. In addition, the high density, stiffness, and chemical stability of WC at elevated temperatures contribute to improved mechanical performance and thermal durability of the composite, making it suitable for demanding engineering applications.

This study investigates the impact of increasing age hardening temperatures, at a constant holding time, on the hardness and wear properties of aluminum–tungsten carbide composites fabricated by stir casting, under three different cooling conditions: furnace cooling, water quenching, and air cooling. The composite samples were aged at 0 °C, 250 °C, and 450 °C for 2 h. The Taguchi method is a statistical optimization technique used to improve process performance by identifying optimal conditions with minimal experimental efforts, when applied to minimize wear rate, it focuses on determining the most effective combination of control factors and their levels that reduce material wear under given conditions.

Materials and methods

Material preparation

In this research, aluminum grade Al7075 was used as the matrix material and tungsten carbide (WC) particles with a particle size of 3–5 µm served as the reinforcement. Aluminium alloy (Al7075) matrix comprises alloying elements of Si, Zn, Cu, Mg, Fe, Cr, Mn and Ti with weight percentages of 5.4, 2.42, 1.42, 0.42, 0.21, 0.13, 0.12 and 0.11, respectively and the remaining composition being aluminum. Al7075-WC composite is manufactured by stir casting technique by incorporating a fixed quantity of 4% wt. of tungsten carbide (WC) to the aluminium matrix[29,30]. The electrical furnace was used to melt the aluminium matrix which was loaded on the crucible furnace at a temperature of 840 ± 10 °C, after the complete melting of the matrix material a tungsten carbide (WC) was added to the molten aluminium, to promote uniform distribution of WC particles within the Al7075 matrix, the reinforcement was preheated to 250 °C before its addition into the molten aluminum. The mixture was then stirred for 2 min at a stirring speed of 200 rpm, which resulted in a satisfactory level of particle dispersion in the

matrix. After complete mixing, the mixture was poured into a mold, and the Al7075/WC parent composite was removed from the mold after cooling.

Experimental methods

Hardness

Specimens for the hardness test, dimensional specification by ASTM E23 standard with length, breadth, and thickness of 55 mm x 10 mm x 10 mm with notch depth and angle of 2 mm and 45° respectively, were meticulously cut from as-cast Al7075/4%wt. WC composite. To prevent cracks, these specimens underwent a thorough polishing process. The effectively homogenize the matrix and improve the performance of the composite during aging, a solutionizing temperature of 530 °C for three hours and then the solutioned composite was quenched in water[31,32]. Subsequently, a composite is subjected to an age hardening process at a temperature of 0 °C (non-aged), 250 °C, and 450 °C for 2 h, with cooling performed under various medium of furnace, water, and atmosphere.

The surface hardness of Al7075/WC composite was investigated by a Brinell hardness testing machine by applying a 500 g load for 30 s. equipped with a steel ball indenter applying a 500 g load for 30 s. Measurements were conducted at three distinct locations on the composite surfaces for both non-aged and age-hardened composites. The comprehensive hardness of Al7075-WC composites was established by calculating the average of the measured hardness values at each aging temperature.

Wear test

For the evaluation of wear, a computerized POD test setup was employed. As per ASTM G99-95 standard, the composite pin measuring 8 mm in diameter and 30 ± 1 mm in length was subjected to wear tests against a counterface made of EN-31 steel[33]. The wear rate of the composite was calculated using Eq. (1), with a systematic variation of the testing parameters, including sliding distances of 1000, 1500, and 2000 m and depression loads of 10 N, 20 N, and 30 N.

$$\text{Wear rate} = \text{Weight loss (gm)} \;/\; (\text{Density (gm/cc)} * \text{Sliding distance (m)}). \tag{1}$$

In adherence to the Taguchi method, an L9 orthogonal design was used to identify the most optimal set of control parameters for both non-aged and aged composites. An EDS image and quantitative results of the Al7075-WC composite are displayed in Fig. 1b and c, which confirms the existence of tungsten carbide (WC) in the composite. Figure 1a illustrates the preparation of a composite pin from parent material to evaluate the wear rate, and Fig. 1d presents the SEM image of tungsten carbide (WC) particles, illustrating their morphology and confirming the particle size range utilized in the study.

X-ray diffraction analysis

X-ray diffraction (XRD) analysis was conducted using a BRUKER D8-QUEST diffractometer to identify the phases present in the Al7075-WC metal matrix composite, including any intermetallic compounds formed during the age-hardening process. Before analysis, the samples were polished to a smooth finish to ensure surface uniformity and remove any residual contaminants. The dimensions of the composite sample used for the XRD analysis were 5 mm × 5 mm × 5 mm.

Fig. 1. (**a**) Tribological testing Al7075-WC composite samples. (**b**) Qualitative result and EDS of Al7075-WC composite samples at different positions from the parent composite. (**c**) SEM and EDS of tungsten carbide reinforcement in the composite samples. (**d**) Particle size of Tungsten Carbide.

Result and discussion

XRD analysis of aluminium/tungsten carbide composite

The XRD analysis of non-aged and aged Al7075/4wt.%WC composite at different temperatures under different cooling environments was conducted to confirm the formation of precipitates. The different intermetallic compounds are formed during ageing and it is highly dependent on the cooling environment and ageing temperature. Figure 2a–g shows the result for XRD of non-aged and age hardened at 250 °C and 450 °C temperature under furnace, water and atmospheric cooled Al7075/4wt.%WC.

The high peak in the XRD result of non-aged Al7075/4wt.%WC composite is Al followed by WC and a significant level of $MgZn_2$ precipitate, shown in Fig. 2a formed due to reaction between internal elements during the melting of aluminium. The precipitates of $MgZn_2$, Mg_2Si, and Al_2Cu form in significant volumes under furnace cooling (FC), as confirmed by the high-intensity peaks observed in the XRD graph presented in Fig. 2b. This results in increased strength properties when aged at 250 °C. However, the peak intensity decreases at an aging temperature of 450 °C shown in Fig. 2c, due to the dissolution of intermetallic compounds in the composite matrix, leading to a reduction in the composite's strength. A similar phenomenon is observed when the composite is aged at 250 °C and 450 °C under water and atmospheric cooling, as represented by the XRD analysis graphs shown in Fig. 2d–g, when the composite is aged at 250 °C under water (WC) and atmospheric cooling (AC). The thickness of the layer between the boundaries increases due to the nucleation of intermetallic compound elements during aging at 250 °C, leading to an increase in the strength of the composite. However, the layer thickness decreases when the composite is aged at 450 °C due to the dissolution of precipitates, resulting in a reduction in strength, regardless of the cooling medium, findings confirmed by Xing Fu et al.[34]. The XRD graph analysis concluded that, during furnace cooling, the composite takes a longer time to reach atmospheric temperature, indicating it remains in the furnace for an extended period. This prolonged exposure promotes increased reactions between the elements in the matrix, leading to the formation of a larger volume of intermetallic compounds, as evidenced by the XRD analysis. Quenching and atmospheric cooling also influence the formation of intermetallic compounds in Al7075-WC composite; however, their effect is less significant compared to furnace cooling.

Hardness

A Brinell hardness machine set up is used to evaluate the hardness value of Al7075/WC composites. This methodological choice not only offers a precise measure of hardness but also provides valuable data on the material's resistance to indentation, thereby contributing to a comprehensive understanding of the composite mechanical properties. Three samples were used to evaluate the hardness under all ageing and cooling circumstances, and an average value was taken. Table 1 presents Brinell hardness of all composite samples under different aging temperatures and cooling environments of non-aged, 250 °C, 450 °C and furnace, water, and atmosphere conditions.

The aged Al7075/4wt.%WC composite under furnace cooling at 250 °C exhibits a higher Brinell hardness number than other aged temperatures in all cooling environments. The eutectic represents the non-faceted phase and it causes to formation structure that increases the strength. The natural property of the α phase is very hard and the natural property of the β phase is soft. The α and β phases appeared in the eutectic reaction. The aged Al7075/4wt.%WC composite at non-aged (0 °C), subjected to the conversion of a small amount of β phase into α phase during the casting process. This occurrence of β phase into α phase is extended up to 250 °C. The ageing temperature at 250 °C, thermodynamic equilibrium occurs and the formation of precipitates is decreased in all kinds of cooling environments.

High hardness is achieved at an aging temperature of 250 °C due to the formation of magnesium and zinc compounds, along with a high volume of Mg_2Si and $MgZn_2$ precipitates and this phenomenon prevents dislocation during loading, thereby enhancing the hardness of the aged Al7075/4 wt% WC composite as compared to water and atmospheric cooled composite as shown in the XRD graph in Fig. 2a. In the diffraction graph analysis of the composite, a high peak (intensity) value indicates that a high volume of precipitates is observed in the composite that undergoes 250 °C under a furnace cooling environment compared to water and atmospheric cooling mediums, which leads to resistance to dislocation under loading and enhanced hardness of the composite. In the temperature range of 250 °C to 450 °C, the hardness of the composite decreased due to the dissolution of precipitates in the aluminum matrix across all cooling environments, indicating over aging. Figure 3. shows the comparison of hardness of the composite at different aging temperatures under furnace, water and atmospheric cooling medium.

Optimization of wear characteristics

The optimization of wear test is done on aged Al7075/4wt.%WC composite at different temperature conditions, applied load, and sliding distances under furnace cooling. The input parameters selected for this optimization are applied load (10 N, 20 N and 30 N), aging temperature (0, 250 °C and 450 °C) and sliding distance (1000 m, 1500 m and 2000 m). The response parameters selected for this investigation are the wear rate of non-aged and aged Al7075/4wt.%WC composite. The L9 orthogonal array is selected for this optimization.

The factor information for optimization is shown in Table 2. The optimization is done to find out the influenced input parameters on the wear rate of composite responses. Taguchi technique optimization is employed for optimizing the input parameters on wear rate responses with the help of Minitab 19 software. The ANOVA is widely used for finding the significance of the input parameters on wear rate responses.

Furnace cooled condition

In furnace cooling, the cooling was done within the furnace after reaching the aging temperature. The L9 orthogonal design table for the furnace-cooled condition of the composite is given in Table 3. It was found that

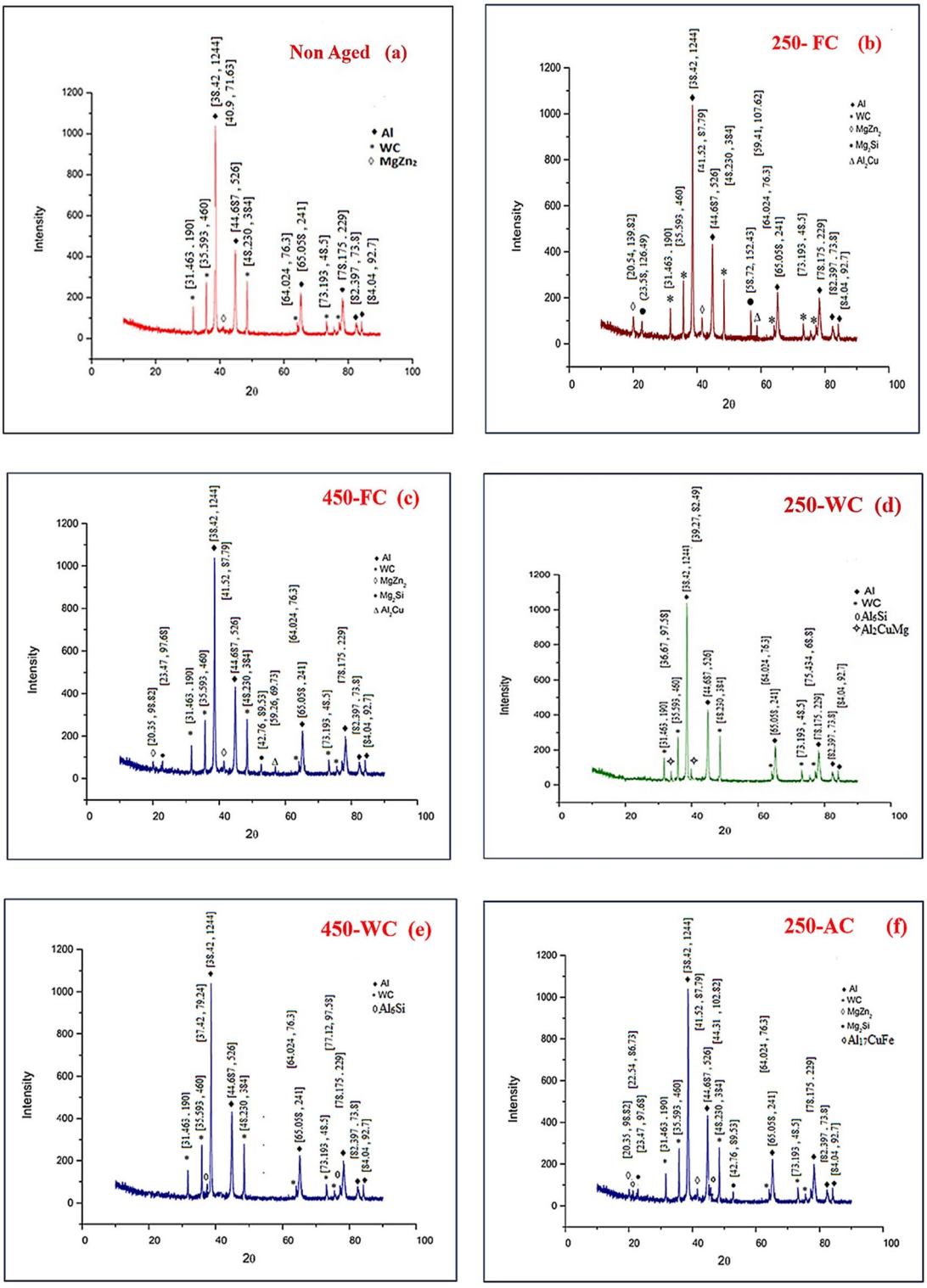

Fig. 2. (**a**–**g**). XRD analysis of (**a**) non-aged (**b**) aged at 250 °C-Furnace cooled (**c**) aged at 450 °C- Furnace cooled (**d**) aged at 250 °C-Water cooled (**e**) aged at 450 °C-Water cooled (**f**) aged at 250 °C- Atmospheric cooled (**g**) aged at 450 °C- Atmospheric cooled.

the maximum and minimum wear rates for the Al7075/WC composite are 0.01174 mm/m³ and 0.00244 mm/m³ for non-aged conditions and aged at 250 °C respectively.

The optimum condition was calculated using a signal-to-noise ratio graph as given in Fig. 4. The "smaller the better" criterion was selected for the optimal condition, as a lower wear rate and increased wear resistance

S. no.	Composite aged for 2 h	Hardness (BHN)		
		Furnace cooling (FC)	Water cooling (WTR)	Atmospheric cooling (ATM)
1	Non aged	83.4	83.4	83.4
2	Aged temperature at 250 °C	125.5	109.1	116.2
3	Aged temperature at 450 °C	121.5	105.8	110.6

Table 1. Brinell hardness of Al7075/WC composite.

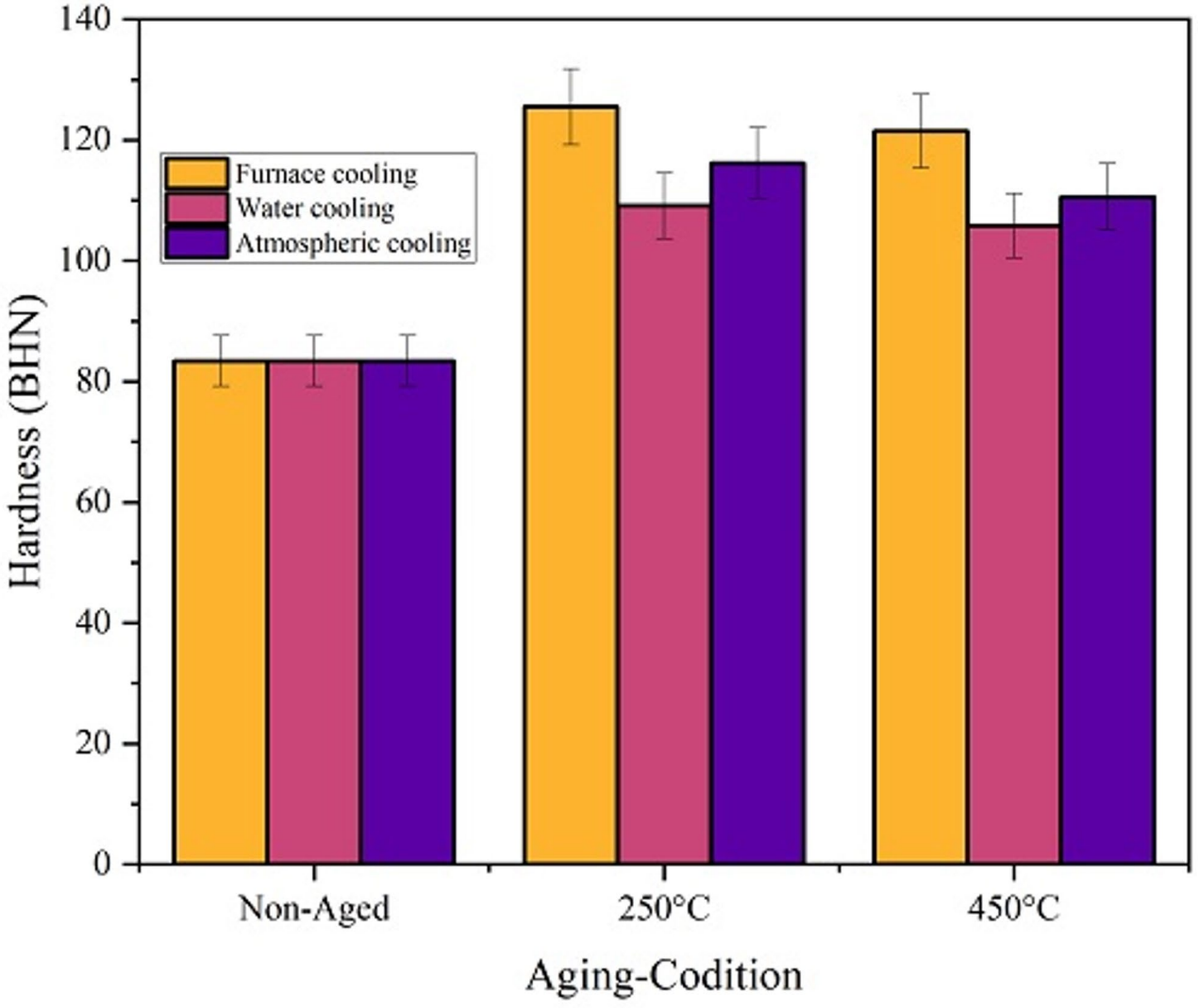

Fig. 3. Comparison of hardness of Al7075-WC composite.

Factor	Name	Units	Levels		
			1	2	3
A	Aging condition	(°C)	0	250	450
B	Load	N	10	20	30
C	Sliding Distance	m	1000	1500	2000

Table 2. Factor information for optimization.

Aging condition	Load (*N*)	Sliding distance (m)	Wear rate (mm/m^3)
Non-Aged	10	1000	0.00754
Non-Aged	20	1500	0.00972
Non-Aged	30	2000	0.01174
250 °C	10	1500	0.00244
250 °C	20	2000	0.00287
250 °C	30	1000	0.00269
450 °C	10	2000	0.00316
450 °C	20	1000	0.00331
450 °C	30	1500	0.00343

Table 3. Design table of Al7075/WC composite under furnace cooled condition.

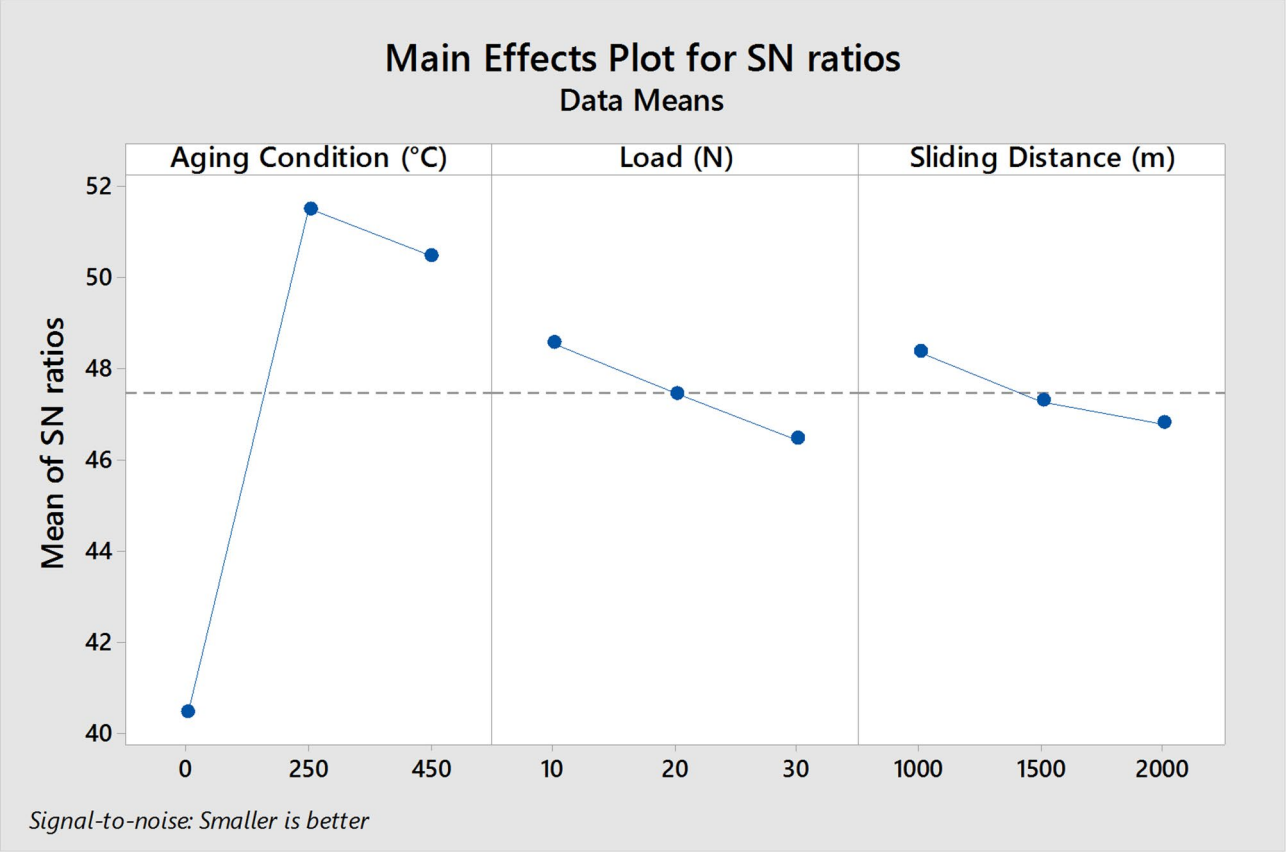

Fig. 4. Signal to noise ratio for furnace cooled condition.

are desirable for industrial applications. The optimum input parameters are aging condition at 250 °C (A2), an applied load of 10 N, and a sliding distance of 1000 m and minimum wear rate, the highlighted condition is best.

The signal to noise ratio table at lower the best condition is given in Table 4. The delta value varies for each input parameter, which ordered the rank of the input factors. The aging condition has a higher delta value so it has the rank 1 followed by load and sliding condition. The aging condition has more influence on the wear rate than other input factors. The highest value was obtained at an aging 250 °C. In this condition, the wear rate decreased due to the formation of hard precipitates with a combination of aluminum and tungsten carbide.

The analysis of variance (ANOVA) table for each input parameter is presented in Table 5. From this table, the significance level of each input parameter can be identified. A low value of the adjusted sum of squares (SS) and adjusted mean square (MS) indicates that the model is significant and has considerable reliability in prediction. The aging temperature shows a 95% confidence level and a 5% significance level. Furthermore, it has a 76.86% R-square value and an 80.97% adjusted R-square value which is somehow closer to 100%. So, the residual value is also pretended to be low. The final regression equation is given in Eq. (2).

Level	Aging condition (°C)	Load (*N*)	Sliding distance (m)
1	40.44	48.54	48.36
2	51.50	47.43	47.26
3	50.47	46.44	46.78
Delta	11.06	2.10	1.57
Rank	1	2	3

Table 4. Signal-to-noise ratio table of Al7075/WC composite under furnace cooled condition.

Source	DF	Adj SS	Adj MS	F-value	*P*-value
Regression	3	0.000079	0.000026	5.66	0.046
Aging condition (°C)	1	0.000072	0.000072	15.36	0.011
Load (N)	1	0.000004	0.000004	0.90	0.386
Sliding distance (m)	1	0.000003	0.000003	0.72	0.436
Error	5	0.000023	0.000005		
Total	8	0.000103			
R^2- value = 76.86%			Adjusted R^2-value = 80.97%		

Table 5. ANOVA table of Al7075/WC composite under furnace cooled condition.

$$\text{Wear Rate } \left(\text{mm/m}^3\right) = 0.00478 - 0.000015 \text{ Aging Condition } (^\circ\text{C}) + 0.000084 \text{ Load (N)} + 0.000001 \text{ Sliding Distance (m)} \quad (2)$$

The response surface graph, shown in Fig. 5, illustrates the interaction effects of the input parameters on the response (wear rate). Load has drastically increased the wear rate as shown in Fig. 5a. It shows the wear rate variation versus load and aging condition for the sliding distance (1500 m) as constant. Aging conditions reduced the wear rate because it increased the surface hardness. In Fig. 5b, the interaction of aging conditions and sliding distance is seen. Here, the load is maintained as constant (20 N). Sliding distance increases with an increase in wear rate but the aging condition changes the phenomenon[35].

The interaction effect also negatively correlates with the response variable. The interaction effect of load and sliding distance increased the wear rate because both influence the wear rate positively, as shown in Fig. 5c. In the beginning, a low wear rate was found because the aging condition was maintained at 233.33 °C, which is an optimum aging condition for a low wear rate.

Atmospheric cooled condition

The aging of Al7075 reinforced with tungsten carbide at atmospheric conditions refers to the changes in the material properties and microstructure that occur over time due to natural aging processes. Aging typically executes the precipitation and growth of strengthening phases within the aluminum matrix, which enhance the material properties. Tribological characterization of prepared sample refers to study about interaction between surfaces in relative motion and, their resulting wear and friction behavior. Here, tribological characterization aims to understand how the addition of WC particles affects the wear rate of the samples. L9 orthogonal array was taken for the analysis as shown in Table 6.

The obtained minimum wear rate is 0.00483 mm/m^3 at an applied load of 10 N, a sliding distance of 1000 m at 250 °C aging temperature, and the maximum wear rate is 0.01174 mm/mm^3 at 30 N load and 2000 m sliding distance under non-aging condition. All the optimum conditions are given in Fig. 6 as named as a signal-to-noise ratio graph. "Smaller is best" was selected for the optimum condition since the lower the wear rate increases the wear resistance which is best for the material industries. In this review, the optimum input parameters are the aging condition at 250 °C (A2), an applied load of 10 N (B1), and the sliding distance of 1500 m (C1). To get a minimum wear rate, the highlighted condition is best. The influence of these factors on the wear rate is significantly considerable.

The impact of each input factor is categorized by ranking method. The rank table based on the signal-to-noise ratio value "smaller is better" condition is given in Table 7. The maximum delta value of 3.87 is obtained in aging conditions. This value varies for each input parameter. So, the aging condition has the rank 1 followed by sliding distance and load. The aging condition has more influence on wear rate than other input parameters such as sliding distance and load. The highest signal-to-noise ratio value was obtained at 1000 m (sliding distance). In this condition, the wear rate value was as low as possible but once it increased the wear rate also increased. It happens due to an increase in the sliding contact time as the sliding distance increases.

The ANOVA table has the raw data from the experiment, including the measurements taken and the corresponding experimental conditions. In this ANOVA Table 8. The calculated F-value and p-value for the input parameter variation are listed. The F-value was obtained by dividing the mean square between treatments by the mean square within treatments. All the p-values represent the significance level of the F-value. Here, except for the aging condition, all are significant because less than 0.05. It was obtained from Minitab statistical

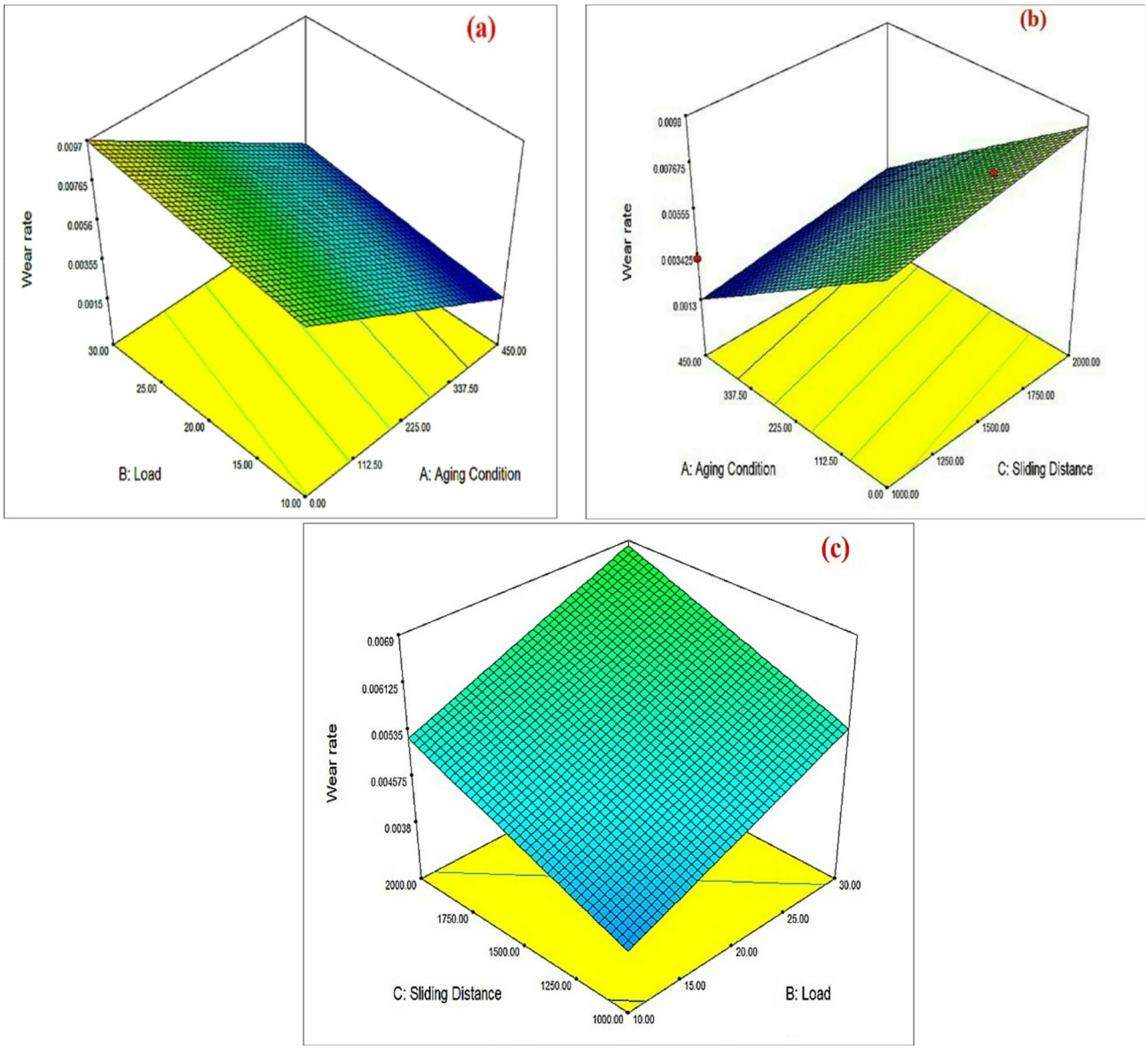

Fig. 5. Response surface graph for furnace cooled condition, (**a**) Interaction between load and Aging condition (**b**) Interaction between Aging condition and sliding distance (**c**) Interaction between sliding distance and load.

Aging condition	Load (*N*)	Sliding distance (m)	Wear rate (mm/m^3)
Non-Aged	10	1000	0.00754
Non-Aged	20	1500	0.00972
Non-Aged	30	2000	0.01174
250 °C	10	1500	0.00483
250 °C	20	2000	0.00522
250 °C	30	1000	0.00563
450 °C	10	2000	0.00683
450 °C	20	1000	0.00758
450 °C	30	1500	0.00789

Table 6. Design table of Al7075/WC composite under atmospheric cooled condition.

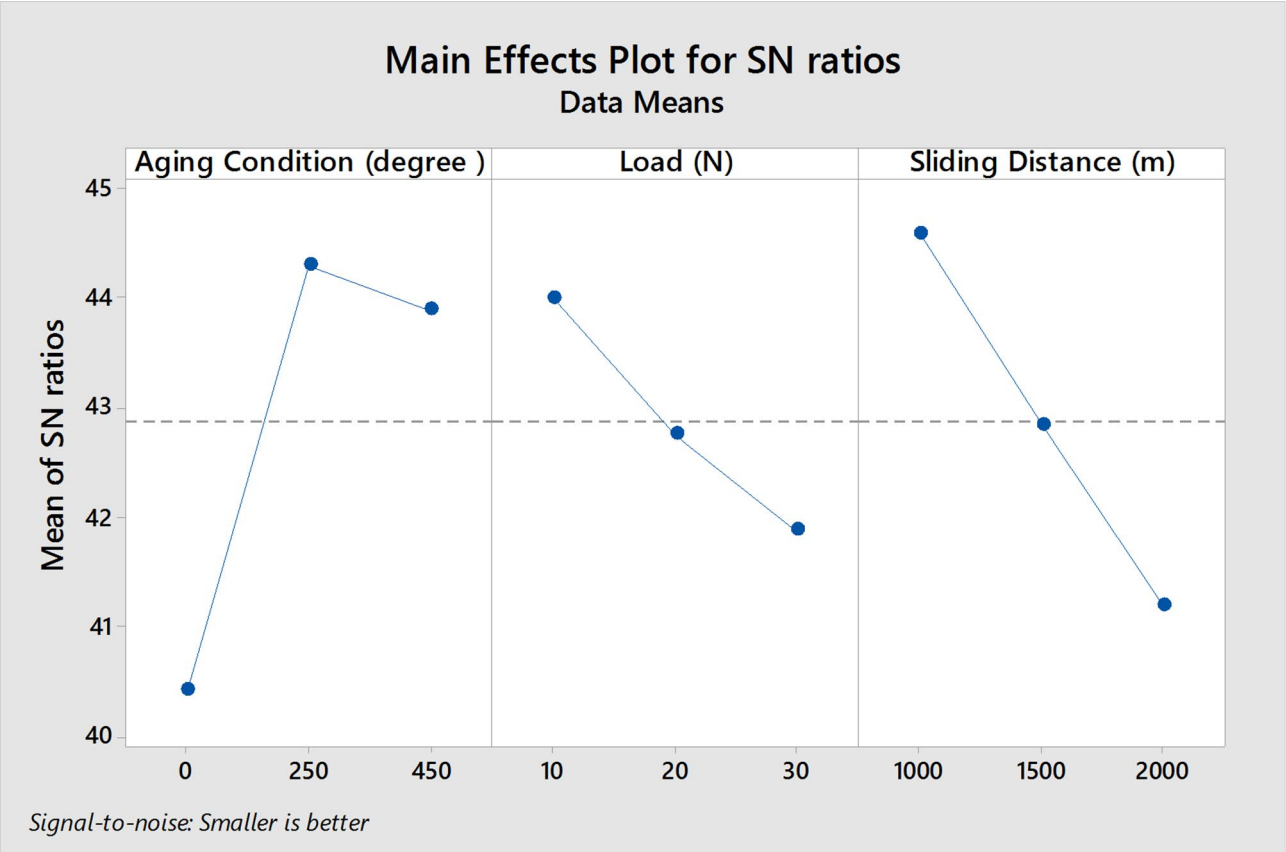

Fig. 6. Signal-to-noise ratio for atmospheric cooled condition.

Level	Aging condition (degree)	Load (*N*)	Sliding distance (m)
1	40.44	44.00	44.59
2	44.31	42.76	42.85
3	43.90	41.88	41.21
Delta	3.87	2.11	3.38
Rank	1	3	2

Table 7. Signal-to-noise ration table of Al7075/WC composite under atmospheric cooled condition.

Source	DF	Adj SS	Adj MS	F-value	*P*-value
Regression	3	0.000035	0.000012	9.02	0.018
Aging Condition (degree)	1	0.000016	0.000016	12.46	0.017
Load (N)	1	0.000006	0.000006	4.65	0.084
Sliding Distance (m)	1	0.000013	0.000013	9.94	0.025
Error	5	0.000006	0.000001		
Total	8	0.000042			
R^2-value = 95.98%			Adjusted R^2-value = 93.57%		

Table 8. ANOVA table of Al7075/WC composite under the atmospheric cooled condition.

software using the degrees of freedom. The R^2-value (95.98%) and Adjusted R^2-value (93.57%) control the high confidence level of the model. The regression Eq. 3 shows a significant coefficient value.

$$\text{Wear Rate } \left(\text{mm/m}^3\right) = 0.00277 - 0.000007 \text{ Aging Condition (degree)} + 0.000100 \text{ Load (N)} + 0.000003 \text{ Sliding Distance (m)} \quad (3)$$

In this analysis, a significant difference is found in wear rate between the maximum level and the minimum level. Figure 7a shows the wear rate variation between aging conditions and sliding distance. Wear rate increased with an increase in load, whereas wear rate decreased with an increase in aging temperature with the decrease in wear rate percentage of decline is significantly considerable which is 31% compared to the high wear rate. In Fig. 7b, the phenomenon is normal as previously. It shows the variation in wear rate when the input parameters, such as aging condition and specific wear rate increased while keeping the load (20 N) constant. Sliding distance increased the wear rate but it was low in the beginning. The aging condition reduced the wear rate. Figure 7c. shows the variation in wear rate when the input parameters, such as load and sliding distance, are changed while keeping the aging condition (250 °C) constant. Low wear was obtained at a minimum load of 10 N and a minimum sliding distance of 1000 m. Further increases were observed when the interaction value was increased[36,37].

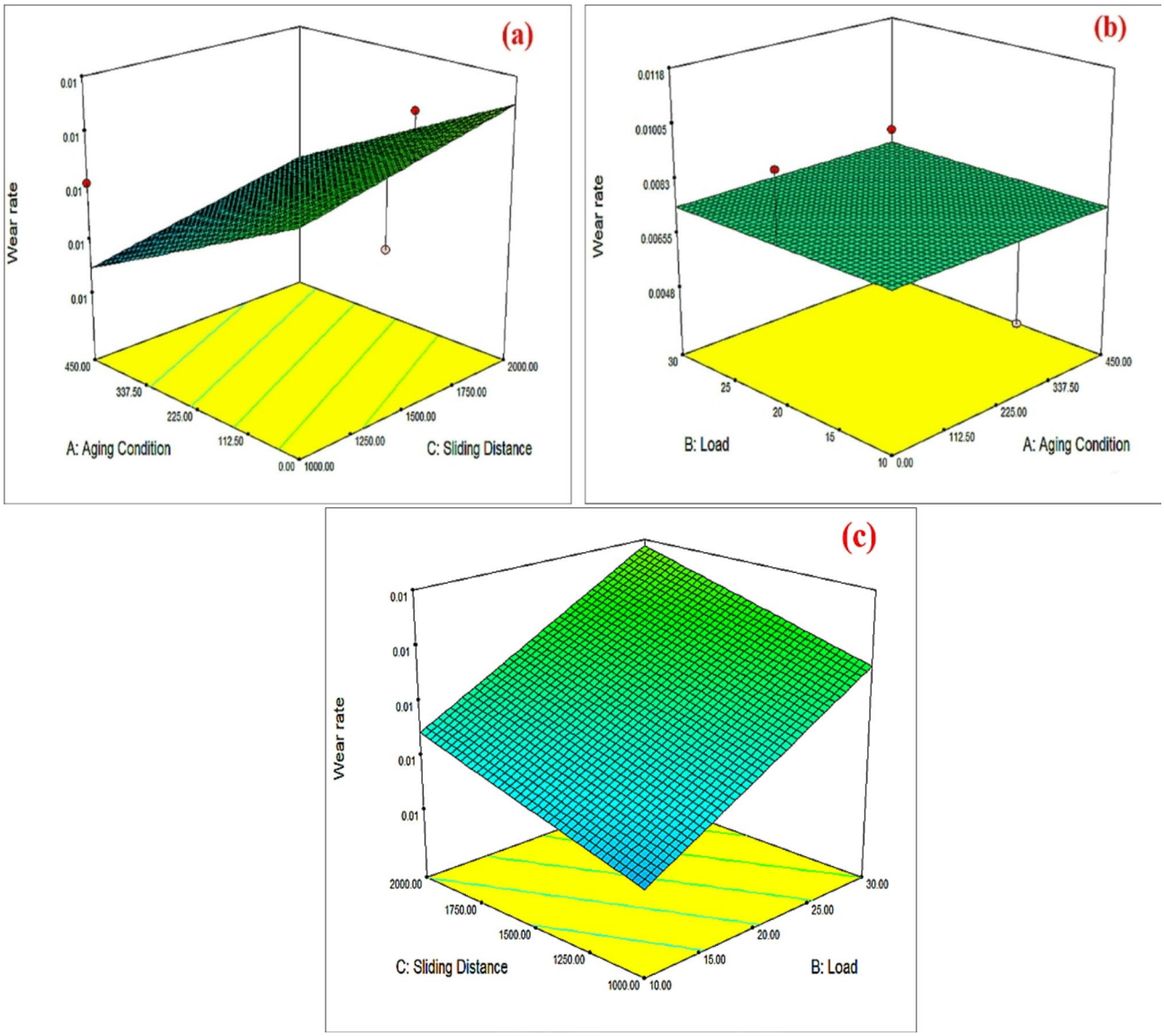

Fig. 7. Response surface graph for atmospheric cooled condition (**a**) Interaction between Aging condition and sliding distance (**b**) Interaction between load and Aging condition (**c**) Interaction between sliding distance and load.

Aging condition	Load (*N*)	Sliding distance (m)	Wear rate (mm/m^3)
Non-Aged	10	1000	0.00954
Non-Aged	20	1500	0.00972
Non-Aged	30	2000	0.01174
250 °C	10	1500	0.00709
250 °C	20	2000	0.0753
250 °C	30	1000	0.00796
450 °C	10	2000	0.00961
450 °C	20	1000	0.00811
450 °C	30	1500	0.00921

Table 9. Design table of Al7075/WC composite under water-cooled condition.

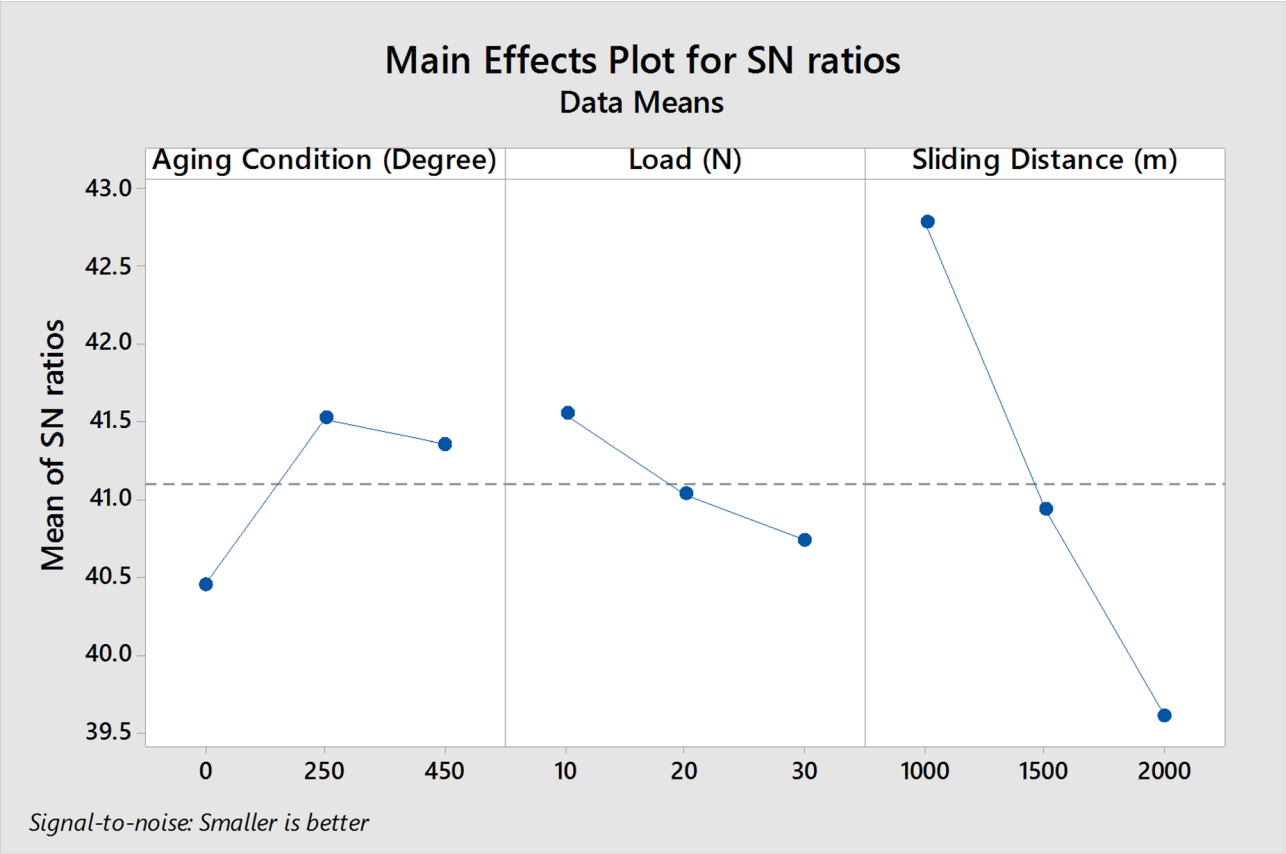

Fig. 8. Signal to noise ratio for water cooled condition.

Water-cooled condition

The prepared material Al7075 reinforced with 4 wt% of Tungsten carbide (WC) composite is heated to 250 and 450 °C and then it is cooled with water. The tribological behavior changes between non-aged and aged with water-cooled have been discussed using Taguchi L9 orthogonal array as shown in Table 9. The obtained minimum wear rate of the composite was 0.00709 mm/m^3 and the maximum value was 0.01174 mm/m^3 as given in the design table. Three factors with three levels have been considered for this study.

The calculated optimum condition using a signal-to-noise ratio graph is given in Fig. 8. "Smaller is best" was selected for the optimum condition since the lower the wear rate increases the wear resistance, which is best for the material industries. As same as in the previous study, the optimum input parameters are the aging condition at 250 °C (A2), an applied load of 10 N (B1), and the sliding distance of 1500 m (C1). To get a minimum wear rate, the highlighted condition is best. The influence of these factors on the wear rate is significant and considerable.

The rank table based on signal-to-noise ratio value "smaller is better" condition is given in Table 10. The delta value varies for each input parameter, which ordered the rank of the input factors. In this study, sliding distance has a higher delta value, so it has the rank 1 followed by aging condition and load.

Level	Aging condition (degree)	Load (*N*)	Sliding distance (m)
1	40.44	41.54	42.77
2	41.51	41.03	40.93
3	41.35	40.73	39.60
Delta	1.08	0.81	3.17
Rank	2	3	1

Table 10. Signal-to-noise ration table of Al7075/WC composite under the water-cooled condition.

Source	DF	Adj SS	Adj MS	F-Value	*P*-value
Regression	3	0.000019	0.000006	38.55	0.001
Aging Condition (Degree)	1	0.000002	0.000002	10.70	0.022
Load (N)	1	0.000001	0.000001	8.50	0.033
Sliding Distance (m)	1	0.000016	0.000016	96.45	0.000
Error	5	0.000001	0.000000		
Total	8	0.000020			
R^2-value = 95.86%			Adjusted R^2-value = 93.37%		

Table 11. ANOVA table of Al7075/WC composite under water cooled condition.

The sliding distance has more influence on wear rate than other input parameters, such as aging condition and load. The highest signal to noise ratio value was obtained at 1000 m (sliding distance). In this condition, it minimized the wear rate but once it increased the wear rate also increased. It happens due to an increase in the sliding contact time as the sliding distance increases. The significance level of each input parameter has been analyzed to get the optimum wear condition. The analysis of variance (ANOVA) table for each input parameter is given in Table 11. The significance level of each input parameter can be identified from this table. The low value of the adjusted sum of squares (SS) and adjusted Mean Square (MS) shows the model is significant and has considerable reliability in the prediction. Aging temperature shows a 95% confidence level and a 5% significance level. Furthermore, it has a 95.86% R-square value and a 93.37% adjusted R-square value, which is somewhat closer to 100%. So, the residual value is also pretended to be low. The final regression equation is given in Eq. (4). The residual value is minimized compared to the previous study. All input parameters have a p-value below 0.05, which means the accuracy level is high. According to the F-value, the influence of sliding distance is high compared to other parameters.

$$\begin{aligned}\text{Wear Rate}\left(\text{mm/m}^3\right) &= 0.003678 - 0.000002\ \text{Aging Condition (Degree)} + 0.000048\ \text{Load (N)} \\ &\quad + 0.000003\ \text{Sliding Distance (m)}\end{aligned} \tag{4}$$

The response surface graph represents a three-dimensional surface on a two-dimensional plane. It is constructed by the connect points of equal value, highlighting levels of interaction or intensity across the surface and the response surface graph is commonly used to visualize data that varies continuously across a surface. The interaction effect of the input parameter on wear rate was studied from a response surface graph. The obtained response surface graph is given in Fig. 9, and the interaction effect of the input parameter on the response (Wear rate) was found in these graphs. In Fig. 9a, the interaction of aging condition and sliding distance is studied by keeping the sliding distance (1500 m) constant. It witnesses of higher wear rate at maximum load conditions but the aging temperature increases with a decrease in wear rate. In Fig. 9b, the load is maintained as constant (20 N), and the aging condition and sliding distance vary within the boundary. Sliding distance increases with an increase in wear rate but the aging condition changes the phenomenon. The interaction effect also has a negative correlation to the response variable. The interaction of load and sliding distance has drastically increased the wear rate as shown in Fig. 9c. Finally, an interaction effect of load and sliding distance increased the wear rate but the value is significantly low. Minimum wear occurs at an age-hardening temperature of 250 °C, while maximum wear is observed at 450 °C, a conclusion also reached by Khoman Kumar et al.[38,39].

Scanning electron microscopic analysis

All three figures exhibit adhesive wear, where the softer aluminum matrix material adheres to the counter surface and then gets torn away during sliding. This is evident in the grooves and scratches that were observed. The severity of the wear decreases as the sliding distance gets shorter (from Fig. 10a to c). This suggests that the wear is most substantial initially and then the wear rate stabilizes.

Figure 10a shows the most extensive wear with deep grooves, debris, and scratches. There are also some areas of microcracking and spalling (chipping) of the tungsten carbide particles. This suggests that the high load and long sliding distance contributed to adhesive wear in the composite[40]. The wear in Fig. 10b is less severe than in Fig. 10a, with shallow grooves and scratches. There is also less evidence of microcracking and spalling. This suggests that the shorter sliding distance led to low wear. Figure 10c shows the least wear, with very fine grooves

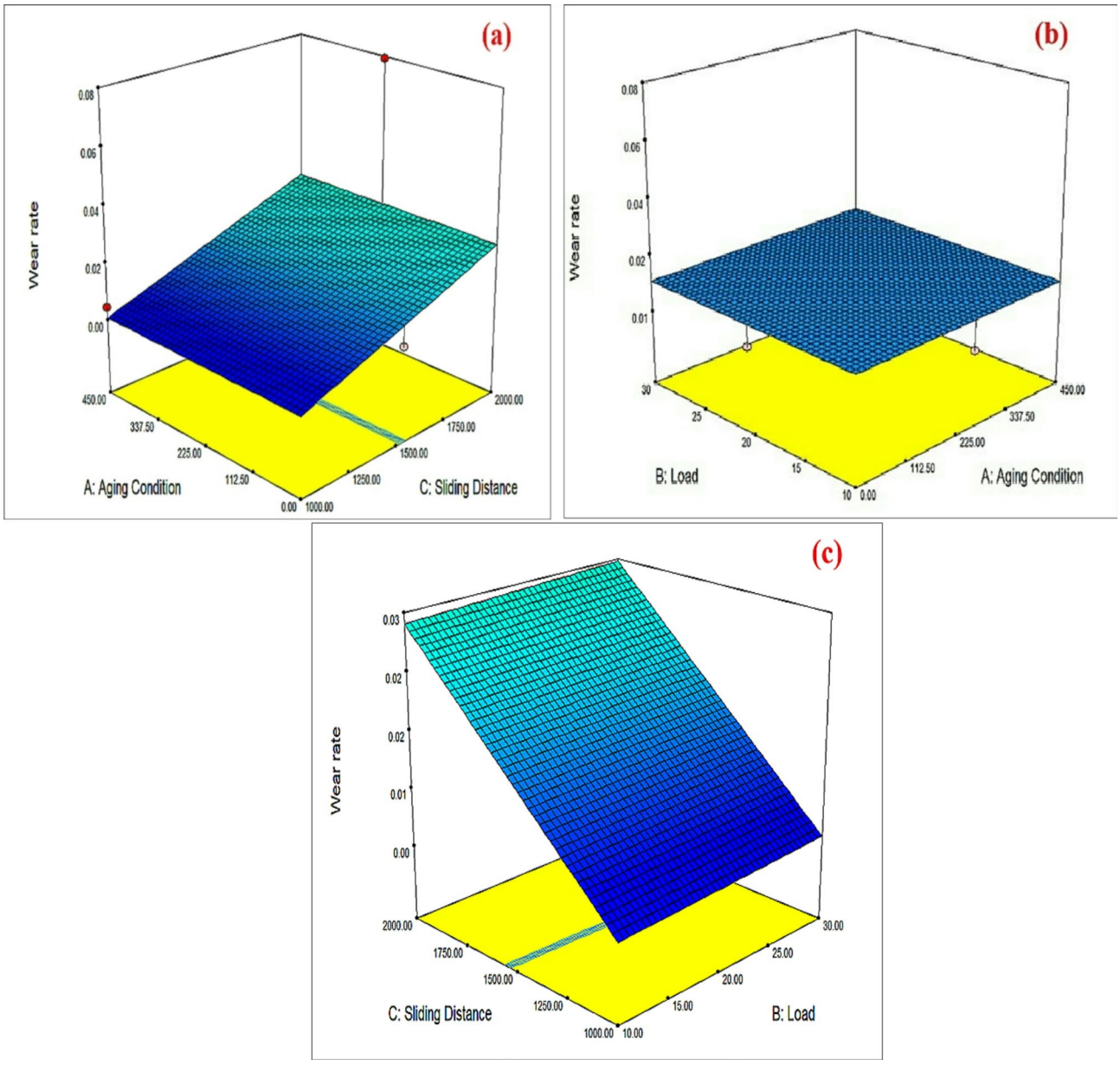

Fig. 9. Response surface graph for water cooled condition (**a**) Interaction between Aging condition and sliding distance (**b**) Interaction between load and Aging condition and load (**c**) Interaction between sliding distance and load.

and scratches and almost no microcracking or spalling. This suggests that the wear is minimal at this load and sliding distance. In conclusion, this study intricate relationship between aging temperature and the tribological behavior of aluminum tungsten carbide composites. The optimization process, guided by the Taguchi method, identified specific conditions that enhance wear resistance under different cooling environments.

The predominant wear mechanism is abrasion, attributed to the presence of hard WC reinforcements and microcrack formation at the particle–matrix interface, whereas plastic deformation becomes more evident under elevated loads or when the aging-induced strengthening of the matrix is insufficient. The overall wear behavior is governed by the combined effect of these mechanisms, which are significantly influenced by the heat treatment conditions, WC particle content, and operational parameters. SEM analysis often shows pitting, deep grooves and smeared layers, especially in samples subjected to higher loads.

Conclusion

The following are the significant outcomes of this study. The constructive and systematic findings are well organized, which were obtained from all the experiments.

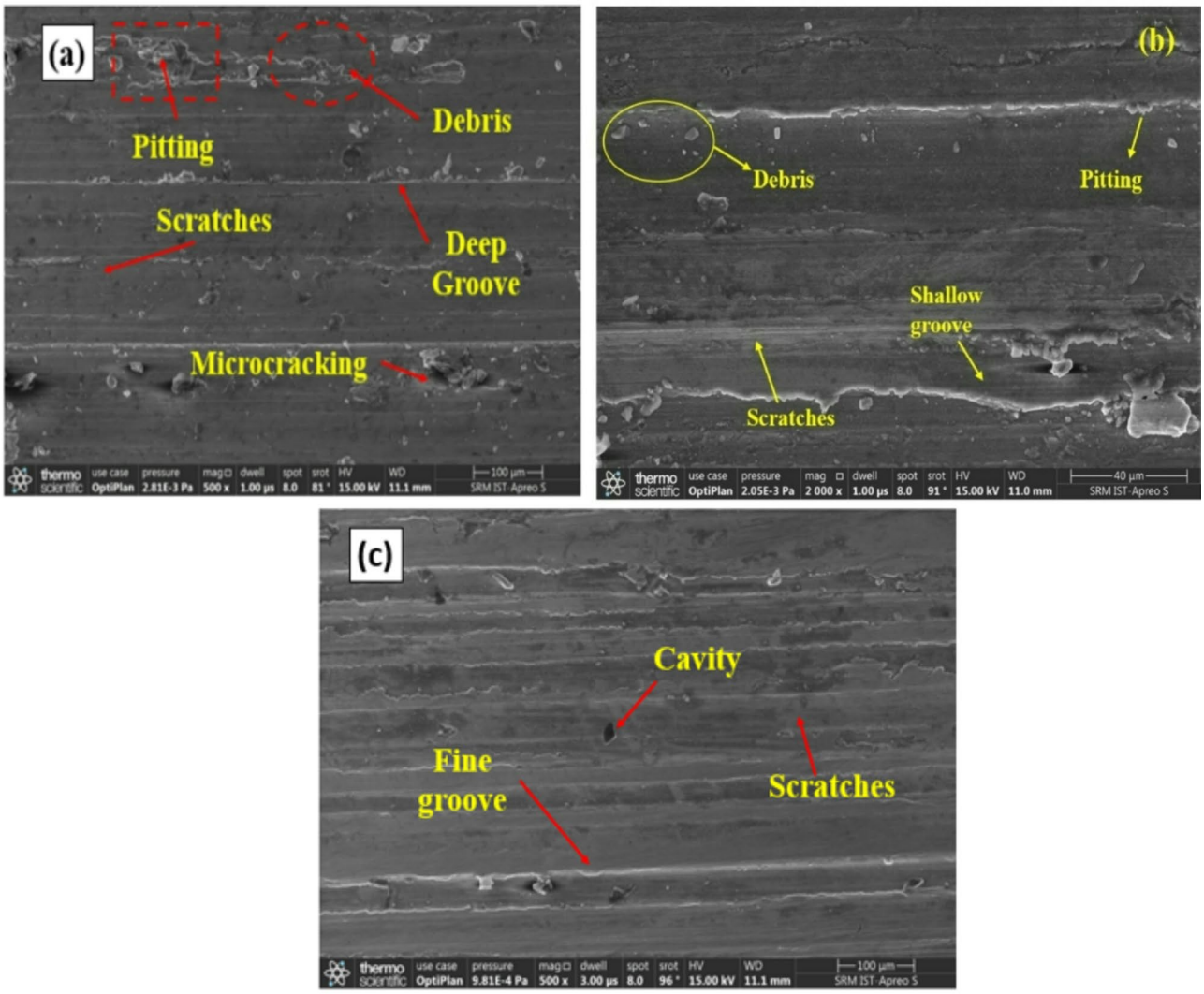

Fig. 10. Worn-out surface after wear test of composite aged at 250 °C under furnace cooled (**a**) Wear condition of 20 N load and 2000 m sliding distance, (**b**) Wear condition of 20 N load and 1500 m sliding distance (**c**) Wear condition of 20 N load and 1000 m sliding distance.

1. The study utilized the Taguchi method to optimize the age-hardening temperature for an aluminum tungsten carbide composite. Three aging temperatures (non-aged, 250 °C, and 450 °C) were considered, and the wear characteristics were investigated using a computerized pin-on-disc test setup.
2. The hardness and wear characteristics of Al7075/WC composite were evaluated under various aging temperatures and cooling environments. The results indicated that aging at 250 °C resulted in the highest hardness and maximum wear resistance compared to other ageing temperatures.
3. The composite aged under furnace cooling at 250 °C exhibited superior hardness due to the formation of precipitates with a higher volume fraction of Mg_2Si and $MgZn_2$, which effectively act as barriers to dislocation motion, thereby enhancing the composite's properties. The aging condition significantly influenced the wear rate, with optimal performance observed at 250 °C.
4. In the XRD analysis, the maximum intensity of peaks was observed in the composite aged at 250 °C, confirming that a higher volume of precipitates was formed compared to other aging temperatures. This results in enhanced strength properties of the Al7075-WC composite across all cooling media.
5. Through optimization, it was determined that the optimum conditions for minimizing wear rate varied based on the cooling environment. For furnace-cooled conditions, aging at 250 °C with a load of 10 N and sliding distance of 1000 m yielded the best results.
6. Similar optimization was performed for atmospheric and water-cooled conditions. For atmospheric cooling, aging at 250 °C with a load of 10 N and a sliding distance of 1000 m was identified as optimal. The study confirms that an increase in load and sliding distance leads to greater wear of the composite.
7. The study demonstrated that the choice of aging temperature significantly impacts the mechanical and tribological properties of the composite. The findings provide valuable insights for materials industries aiming to

enhance wear resistance. Further research could explore additional parameters and real-world applications of the optimized composite.

8. The SEM observations suggest that adhesive wear is the primary mechanism in these samples. The severity of the wear is influenced by the load, sliding distance, and possibly the age-hardening temperature of the composite.

Data availability

The datasets used and/or analysed during the current study available from the corresponding author on reasonable request.

Received: 20 March 2025; Accepted: 4 June 2025
Published online: 01 July 2025

References

1. Kumar, G. S. P., Koppad, P. G., Alipour, M. & Ramaiah Keshavamurthy & Microstructure and mechanical behaviour of in situ fabricated AA6061-TiC metal matrix composites. *Archives Civil Mech. Eng.* **17**, 535–544 (2017).
2. Gurpreet, S. & Goyal, S. Dry sliding wear behaviour of AA6082-T6/SiC/B4C hybrid metal matrix composites using response surface methodology. *J. Materials: Des. Appl.*, 1–13. (2016).
3. Karthik, M., Sharma, S., Gowrishankar, M. C. & Hegde, A. Peak hardness stability analysis of Al7075 alloy dispersed with Ni coated Duralumin powder during natural aging phenomena. *J. Mater. Res. Technol.* **26**, 2219–2228 (2023).
4. Gopalakrishnan, N. M. Production and wear characterisation of AA 6061 matrix titanium carbide particulate reinforced composite by enhanced stir casting method. *Compos. Part. B: Eng.* **43**, 302–308 (2012).
5. Rajaram, S., Subbiah, T., Mahali, P. K. & Thangaraj, M. Effect of age hardening temperature on mechanical and wear behavior of furnace-cooled Al7075-tungsten carbide composite. *Materials* **15**, 5344–5365 (2022).
6. Ramesh, S. Safiulla Wear behavior of hot extruded Al6061 based composites. *Wear* **263**, 629–635 (2007).
7. Liu, Y., Chen, W., Yang, C., Zhu, D. & Li, Y. Effects of metallic Ti particles on the aging behavior and the influenced mechanical properties of squeeze-cast (SiC-Ti)/7075Al hybrid composites. *Mater. Sci. Eng. A*. **620**, 190–197 (2014).
8. Natrayan, L. & Senthil Kumar, M. Optimization of wear behaviour on AA6061/Al2O3/SiC metal matrix composite using squeeze casting technique. *Stat. Anal. Mater. Today*. **27**, 306–310 (2020).
9. Sahin, Y. Optimization of testing parameters on the wear behaviour of metal matrix composites based on the Taguchi method. *Mater. Today*. **408**, 1–8 (2005).
10. Rajeshkumar, L. et al. Optimization of wear behaviour for AA2219-MoS2 metal matrix composites in dry and lubricated condition. *Mater. Today*. **27**, 2645–2649 (2020).
11. Joiet Joseph, B. S. et al. Shankar mechanical behaviour of age hardened A356/TiC metal matrix composite. *Mater. Today* **38**, 2127–2132 (2021).
12. Raju, K. & Balakrishnan, M. Dry sliding wear behavior of aluminum metal matrix composite reinforced with lithium and silicon nitride silicon. **14**, 115–125 (2022).
13. Bharathi, P. & Sampath Kumar, T. Mechanical characteristics and wear behaviour of al/sic and al/sic/B4C hybrid metal matrix composites fabricated through powder metallurgy route silicon. **15**, 4259–4275 (2023).
14. Manu Sam, N., Radhika, M., Ramu, B. & Saleh Alokesh Pramanik optimizing reciprocal wear responses of centrifugally cast A333 hybrid functionally graded composite using Taguchi and response surface methodology. *Int. J. Interact. Des. Manuf.*, 1323–1338. https://doi.org/10.1007/s12008-022-01125-3 (2023).
15. Rajesh, A. M., Kaleemulla, M. & Bharath, S. Material characterization of SiC and Al2O3–reinforced hybrid aluminum metal matrix composites on wear behavior. *J. Mech. Sci. Technol.* **32**, 3123–3128 (2018).
16. Bandhu, D., Thakur, A. & Purohit, R., Rajesh Kumar, V. & Kumar, A. characterization & evaluation of Al7075 MMCs reinforced with ceramic particulates and influence of age hardening on their tensile behavior. *J. Mech. Sci. Technol.* **32**, 3123–3128 (2018).
17. Vembu, V. & Ganesan, G. Heat treatment optimization for tensile properties of 8011 al/15% SiCp metal matrix composite using response surface methodology. *Def. Technol.* **11**, 390–395 (2015).
18. Singh, G. & Goyal, S. Microstructure and mechanical behaviour of AA6082-T6/SiC/B4C based aluminium hybrid composites. *Part. Sci. Technol.* https://doi.org/10.1080/02726351.2016.1227410
19. Gireesh, C. H. Durga Prasad and Koona Ramji experimental investigation on mechanical properties of an Al6061 hybrid metal matrix composite. *J. Compos. Sci.* **2**, 49. https://doi.org/10.3390/jcs2030049 (2018).
20. Swapna, B., Prasad, D., Darla, V. R. & Chokka, S. K. Numerical and experimental analysis of Al6082 composites reinforced with TiB2 and MWCNT for enhanced mechanical properties. *Int. J. Interact. Des. Manuf. (IJIDeM)*, 4247–4253. https://doi.org/10.1007/s12008-024-02000-z (2024).
21. Tang, S. et al. Jie teng microstructure and mechanical behaviors of 6061 al matrix hybrid composites reinforced with SiC and stainless steel particles. *Mater. Sci. Eng. A*. **804**, 140732 (2021).
22. Subramanya Reddy, P., Kesavan, R. & Vijaya Ramnath, B. Investigation of mechanical properties of aluminium 6061-silicon carbide, boron carbide metal matrix composite silicon. **10**, 495–502. https://doi.org/10.1007/s12633-016-9479-8 (2018).
23. Suresh, S., Harinath Gowd, G. & Deva Kumar, M. L. S. Mechanical properties of AA 7075/Al2O3/SiC Nano-metal matrix composites by Stir-Casting method. *J. Inst. Eng. India Ser. D*. https://doi.org/10.1007/s40033-019-00178-1 (2019).
24. Zhu, J., Jiang, W., Li, G. & Guan, F. Zitian fan microstructure and mechanical properties of SiCnp/Al6082 aluminum matrix composites prepared by squeeze casting combined with stir casting. *J. Mater. Process. Tech.* **283**, 116699 (2020).
25. Kalkanl, A. & Yılmaz, S. Synthesis and characterization of aluminum alloy 7075 reinforced with silicon carbide particulates. *Mater. Des.* **29**, 775–780 (2008).
26. Venkatesh, V. S. S. Deoghare microstructural characterization and mechanical behaviour of SiC and kaoline reinforced aluminium metal matrix composites fabricated through powder metallurgy technique. *Silicon* https://doi.org/10.1007/s12633-021-01154-9 (2021).
27. Kumaran, M. et al. Influence of heat treatment on stainless steel 316L alloy fabricated using directed energy deposition. *Mater. Today: Proc.* **62**, 5307–5310 (2022).
28. Sathies, T. et al. Investigations on the effect of heat treatment on laser powder bed fusion built SS316L alloy. *Mater. Today: Proc.* **62**, 5411–5414 (2022).
29. Krishna, A. R., Arun, A., Unnikrishnan, D. & Shankar, K. V. An investigation on the mechanical and tribological properties of alloy a356 on the addition of WC. *Mater. Today Proc.* **5**, 12349–12355. https://doi.org/10.1016/j.matpr.2018.02.213 (2018).
30. Ravikumar, K., Kiran, K. & Sreebalaji, V. S. Characterization of mechanical properties of aluminium/tungsten carbide composites. *Measurement* **102**, 142–149. https://doi.org/10.1016/j.measurement.2017.01.045 (2017).
31. Vembu, V. & Ganesan, G. Heat treatment optimization for tensile properties of 8011 al/15% SiCp metal matrix composite using response surface methodology. *Def. Technol.* **11**, 390–3952. https://doi.org/10.1016/j.dt.2015.03.004 (2015).

32. Ravinath, H. et al. Impact of aging temperature on the metallurgical and dry sliding wear behaviour of LM25/Al2O3 metal matrix composite for potential automotive application. *Int. J. Lightweight Mater. Manuf.* (6), 416–433. https://doi.org/10.1016/j.ijlmm.2023.01.002 (2023).
33. Kang, A. S. & Cheema, G. S. Shivali SinglaWear behavior of hardfacings on rotary tiller blades. *Procedia Eng.* **97**, 1442–1451 (2014).
34. Fu, X., Wang, R., Zhu, Q., Wang, P. & Zuo, Y. Effect of annealing on the interface and mechanical properties of Cu-Al-Cu laminated composite prepared with cold rolling. *Materials* https://doi.org/10.3390/ma13020369 (2020).
35. Surya, M. S. Optimization of machining parameters while turning AISI316 stainless steel using response surface methodology. *Sci. Rep.* **14**, 1–12 (2024).
36. Surya, M. S., Prasanthi, G., Kumar, A. K., Sridhar, V. K. & Gugulothu, S. K. Optimization of cutting parameters while turning Ti-6Al-4 V using response surface methodology and machine learning technique. *Int. J. Interact. Des. Manuf. (IJIDeM)*. **15**, pp453–462 (2021).
37. Surya, M. S., Prasanthi, G. & Gugulothu, S. K. Investigation of mechanical and wear behaviour of Al7075/SiC composites using response surface methodology. *Silicon* **13**, 2369–2379 (2021).
38. Kumar, K., Dabade, B. M., Wankhade, L. N., Agrawa, E. & Chavhan, G. Experimental investigation on tribological performance and development of wear prediction equation of aluminium composite at elevated temperatures. *Int. J. Interact. Des. Manuf. (IJIDeM)*, 1979–1987. https://doi.org/10.1007/s12008-022-00911-3 (2024).
39. Elvin, R. P. et al. Experimental investigation of bead geometry and tribological analysis of IN718 Precipitation-Hardened alloy synthesized by wire Arc additive manufacturing. *J. Mater. Eng. Perform.* (2024).
40. Siva Surya, M., Prasanthi, G. & Gugulothu, S. K. Investigation of mechanical and wear behaviour of Al7075/SiC composites using response surface methodology. *Silicon* https://doi.org/10.1007/s12633-020-00854-y (2021).

Acknowledgements

The authors extend their appreciation to Taif University, Saudi Arabia, for supporting this work through project number (TU-DSPP-2024-32).

Author contributions

Srinivasan Rajaram : Conceptualisation, writing original draft, review, and editing., N.S.B: Supervision, review, and editing., Mamdooh Alwetaishi: supervision; Shashikumar Krishnan: review and editing, formatting.

Funding

The authors extend their appreciation to Taif University, Saudi Arabia, for supporting this work through project number (TU-DSPP-2024-32).

Declarations

Competing interests

The authors declare no competing interests.

Additional information

Correspondence and requests for materials should be addressed to S.R. or S.K.

Reprints and permissions information is available at www.nature.com/reprints.

Publisher's note Springer Nature remains neutral with regard to jurisdictional claims in published maps and institutional affiliations.